3.10. ACCURACY IN RIETVELD QUANTITATIVE PHASE ANALYSIS

the ALBA Light Source (Fauth *et al.*, 2013). The wavelength, λ = 0.77439 (2) Å, was selected with a double-crystal Si(111) monochromator and was determined using the NIST SRM640d Si standard (a = 5.43123 Å). The diffractometer is equipped with a MYTHEN-II detector system. The samples were loaded into glass capillaries 0.7 mm in diameter and were rapidly rotated during data collection to improve the diffracting-particle statistics. The data-acquisition time was 20 min per pattern to attain a very good signal-to-noise (S/N) ratio over the angular range 1–35° 2θ. Three patterns, taken at different positions along the capillaries, were collected for each sample.

SXRPD data for the amorphous content series, CZQ_*x*Gl, were also measured at the ALBA Light Source. The experimental setup was the same as described above but the working wavelength was λ = 0.49591 (2) Å.

#### 3.10.4. Powder-diffraction data analysis

All powder patterns were analysed by the Rietveld method using the *GSAS* software package (Larson & Von Dreele, 2000) with the pseudo-Voigt peak-shape function (Thompson *et al.*, 1987) for RQPA. The refined overall parameters were phase scale factors, background coefficients (linear interpolation function), unit-cell parameters, zero-shift error, peak-shape parameters and preferred-orientation coefficient, when needed. The March–Dollase preferred-orientation adjustment algorithm was employed (Dollase, 1986). The modelling direction must be given as input for the calculations. In this case, the directions for the different phases were taken from previous studies. Alternatively, this direction can be extracted from the pattern from an analysis of the differences between observed and calculated intensities for non-overlapped diffraction peaks. The crystal structures used are reported in Table 3.10.1.

In order to provide a single numerical assessment of the performance of each analysis, a statistic based on the KLD distance was used (Kullback, 1968). This approach was previously used to evaluate the accuracy of RQPA applied to standard mixtures (Madsen *et al.*, 2001; Scarlett *et al.*, 2002; León-Reina *et al.*, 2009). Both phase-related KLD distances and absolute values of the Kullback–Leibler distance (AKLD) were calculated. Accurate analyses are mirrored by low values of AKLD.

The overall amorphous content was determined from the internal standard methodology approach (De la Torre *et al.*, 2001; Aranda *et al.*, 2012) with quartz as an internal standard [using isotropic atomic displacement parameters (ADPs) of 0.045 and 0.0087 Å^2 for Si and O, respectively]. If the original sample contains an amorphous phase, the amount of standard will be overestimated in RQPA. From the (slight) overestimation of the standard, the amorphous content of the investigated sample can be derived (De la Torre *et al.*, 2001). The important role of the values of the ADPs in the results of RQPA mainly in amorphous content determinations using the internal-standard method has been discussed previously (Madsen *et al.*, 2011).

3.10.5. Crystalline single phases

All of the single phases were selected according to several parameters, such as relevance to selected applications, purity, particle size of the powder and preferred orientation. In order to check the suitability of the crystal structures used, all of the phases were first studied using powder diffraction with Mo $K\alpha_1$ radiation. These preliminary studies were of special interest for organic phases, as the CIF files obtained from the Cambridge
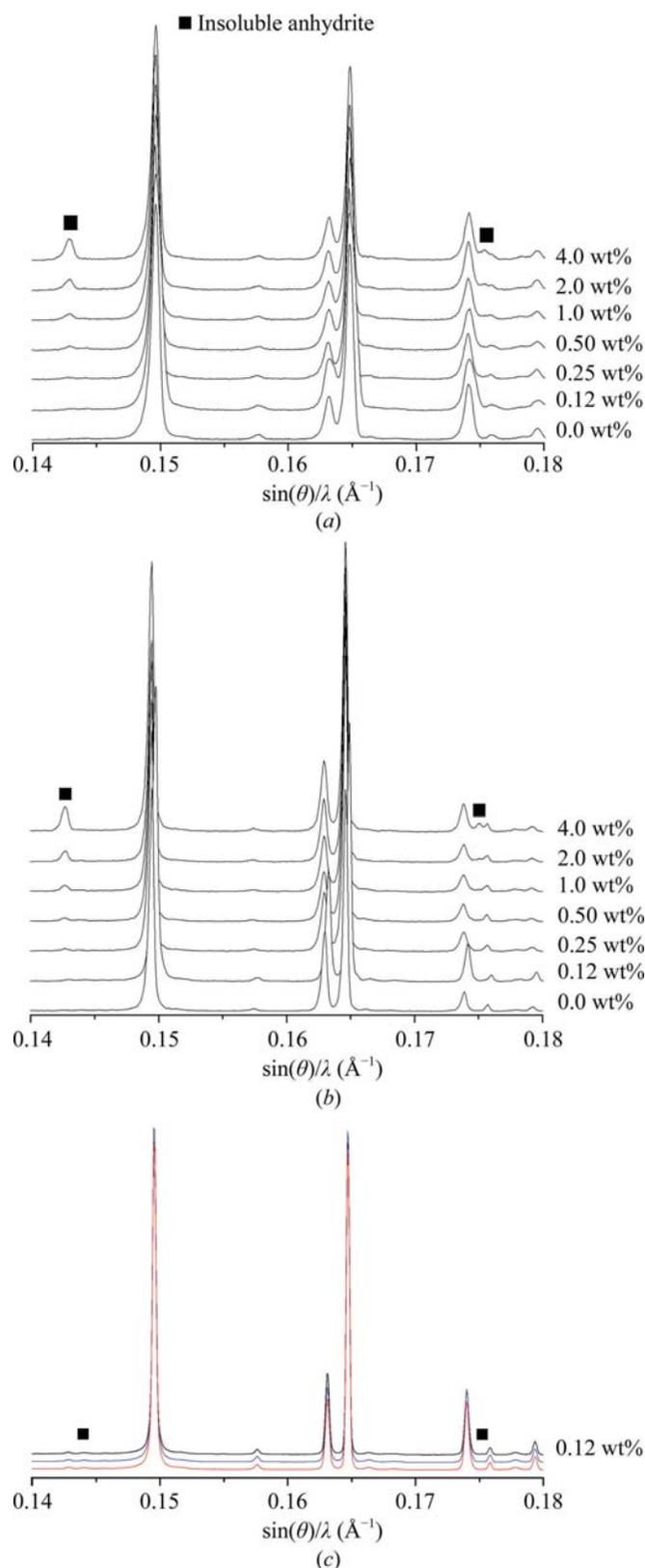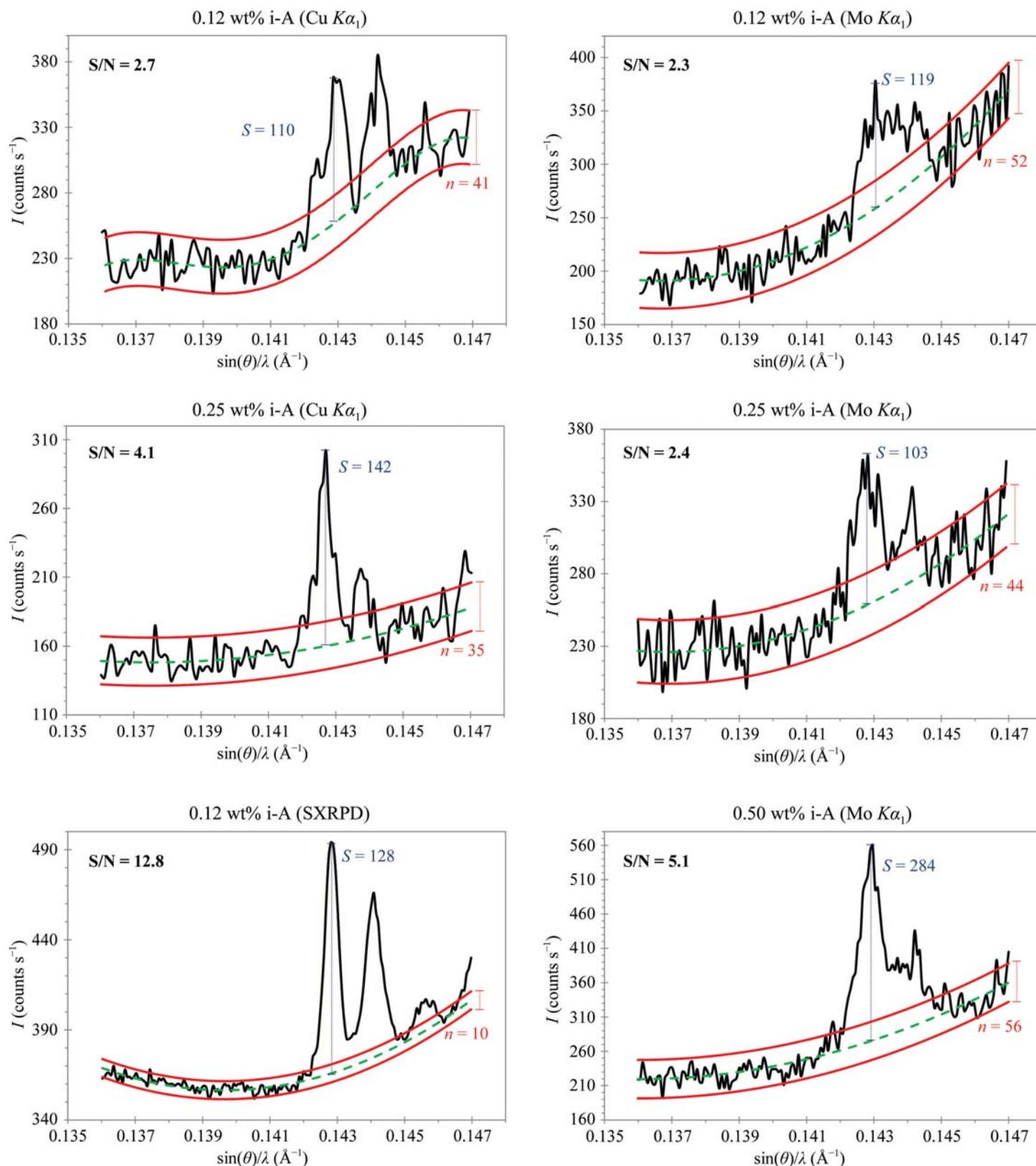
Figure 3.10.3
(*a*) Raw Mo $K\alpha_1$ powder patterns for the inorganic series composed of a constant matrix of calcite, gypsum and quartz, and increasing amounts of insoluble anhydrite (peaks highlighted with a solid square). (*b*) Raw Cu $K\alpha_1$ powder patterns for the same inorganic series. (*c*) Raw SXRPD patterns for CGpQ_0.12A collected at three different positions of the capillary (red, black and blue traces). The intensity values in (*c*) have been artificially offset to show the three different patterns.

Structural Database (CSD) did not contain the atomic displacement parameters (ADPs). For lactose and fructose, the ADPs were obtained from the original publications and were introduced manually into the *GSAS* control file. For glucose and

Figure 3.10.4

Selected region of the powder patterns showing the main diffraction peak of insoluble anhydrite for the low-content samples to investigate the limit of detection. Top left: Cu $K\alpha_1$ pattern for CGpQ_0.12A. Middle left, Cu $K\alpha_1$ pattern for CGpQ_0.25A. Bottom left, SXRPD pattern for CGpQ_0.12A. Top right, Mo $K\alpha_1$ pattern for CGpQ_0.12A. Middle right, Mo $K\alpha_1$ pattern for CGpQ_0.25A. Bottom right, Mo $K\alpha_1$ pattern for CGpQ_0.50A. The main peak of anhydrite, $(\theta)/\lambda = 0.143$ Å^{-1}, is located at 25.4, 11.6 and 12.7° 2θ for Cu $K\alpha_1$, Mo $K\alpha_1$ and synchrotron radiations, respectively. The peak at $\sin(\theta)/\lambda = 0.1445$ Å^{-1} is due to the soluble anhydrite from gypsum (constant content in all the samples). The very tiny peak at $\sin(\theta)/\lambda = 0.1457$ Å^{-1}, which is slightly visible only in the SXRPD pattern, arises from $SrSO_4$ (0.39 wt%) from gypsum.

xylose, the ADP values were not reported in the original publications. Hence, they were obtained from the fits to the Mo $K\alpha_1$ patterns for the single phases. Three groups of isotropic ADPs were refined: those for O, C and H atoms. The final ADP values are given in León-Reina *et al.* (2016) as well as the R_F values

before and after optimization, showing the improvements in the fits. For RQPA of all of the mixtures the ADPs were kept fixed.

Preferred orientation was modelled by the March–Dollase algorithm along the [001] axis for both glucose and lactose. Since microparticle sizes and distributions for different phases may

result in some sample-related effects, such as preferred orientation, microabsorption and 'rock-in-the-dust/graininess' effects, all powders were characterized by scanning electron microscopy (SEM). Fig. 3.10.2 shows SEM micrographs for all of the phases. All inorganic samples were single phases except for gypsum and insoluble anhydrite. The impurity-phase contents for these two samples were reported in León-Reina *et al.* (2016).

Both organic and inorganic phases were also measured using Cu $K\alpha_1$ radiation in reflection mode. As expected, a transparency effect was observed in the Cu $K\alpha_1$ patterns for organic samples (Buhrke *et al.*, 1998).

### 3.10.6. Limits of detection and quantification

LoD and LoQ are two important quantities in the validation of any analytical method. LoD/LoQ are terms that are used to describe the smallest concentration of an analyte that can be reliably detected/assessed by an analytical procedure, as discussed in Section 3.10.1. In techniques such as Rietveld analysis, the approach of having a powder pattern with its strongest (not overlapped) diffraction peak with an S/N ratio of larger than 3.0 is not straightforward because the full powder pattern is evaluated.

Fig. 3.10.3 shows Mo $K\alpha_1$ and Cu $K\alpha_1$ raw patterns for the inorganic series with increasing amounts of insoluble anhydrite (labelled with solid squares) and Fig. 3.10.4 shows the strongest diffraction peak for i-A in the mixtures containing 0.123 wt% anhydrite (CGpQ_0.12A) and 0.25 wt% anhydrite (CGpQ_0.25A) to evaluate the limits of detection in the conditions reported in Section 3.10.5. For CGpQ_0.12A, both laboratory powder patterns yielded peaks with S/N ratios lower than 3.0 (top panels in Fig. 3.10.4). For CGpQ_0.25A, the Cu $K\alpha_1$ pattern yielded a clear peak with S/N = 4.1; therefore, it can be concluded that the LoD for insoluble anhydrite with this radiation in this mixture is slightly lower than 0.2 wt%. For Mo $K\alpha_1$ radiation, the CGpQ_0.25A and CGpQ_0.50A samples yielded patterns with peaks with S/N ratios of 2.4 and 5.1, respectively. Hence, it can be concluded that the LoD for i-A with this radiation in this mixture is quite close to 0.3 wt%.

The LoQ for i-A in this matrix was also studied. Three Mo $K\alpha_1$ and Cu $K\alpha_1$ patterns were collected for CGpQ_0.12A. For the three Mo $K\alpha_1$ patterns, the average analysis result for i-A was 0.28 (2) wt%, but the accuracy of the obtained value is poor, as the expected value was 0.12 wt%. Similarly, the average value for the analyses of three Cu $K\alpha_1$ patterns was 0.24 (2) wt%. The RQPA results are given as supporting information in León-Reina *et al.* (2016). It was concluded that i-A can be quantified in this mixture at the level of 0.12 wt%, but with a relative error close to 100%. If the 'acceptable reliability' criterion in the analysis is taken into consideration, the LoQ value would be close to 1.0 wt% in order to have a relative associated error lower than 20%.

CGpQ_0.12A was also studied by SXRPD. Fig. 3.10.3(*c*) shows the SXRPD patterns collected at three different positions of the capillary, which were almost identical, and Fig. 3.10.4 (bottom left) shows the main diffraction peak of anhydrite. The S/N ratio for the strongest diffraction peak of anhydrite was 12.8 and hence the limit of detection for i-A with synchrotron radiation in this matrix is below 0.10 wt%.

To quantify the accuracy of the analyses, the KLD methodology was used. The AKLD values for each analysis as well as the KLD values for i-A are reported in León-Reina *et al.* (2016). The synchrotron analyses clearly had better accuracy than those
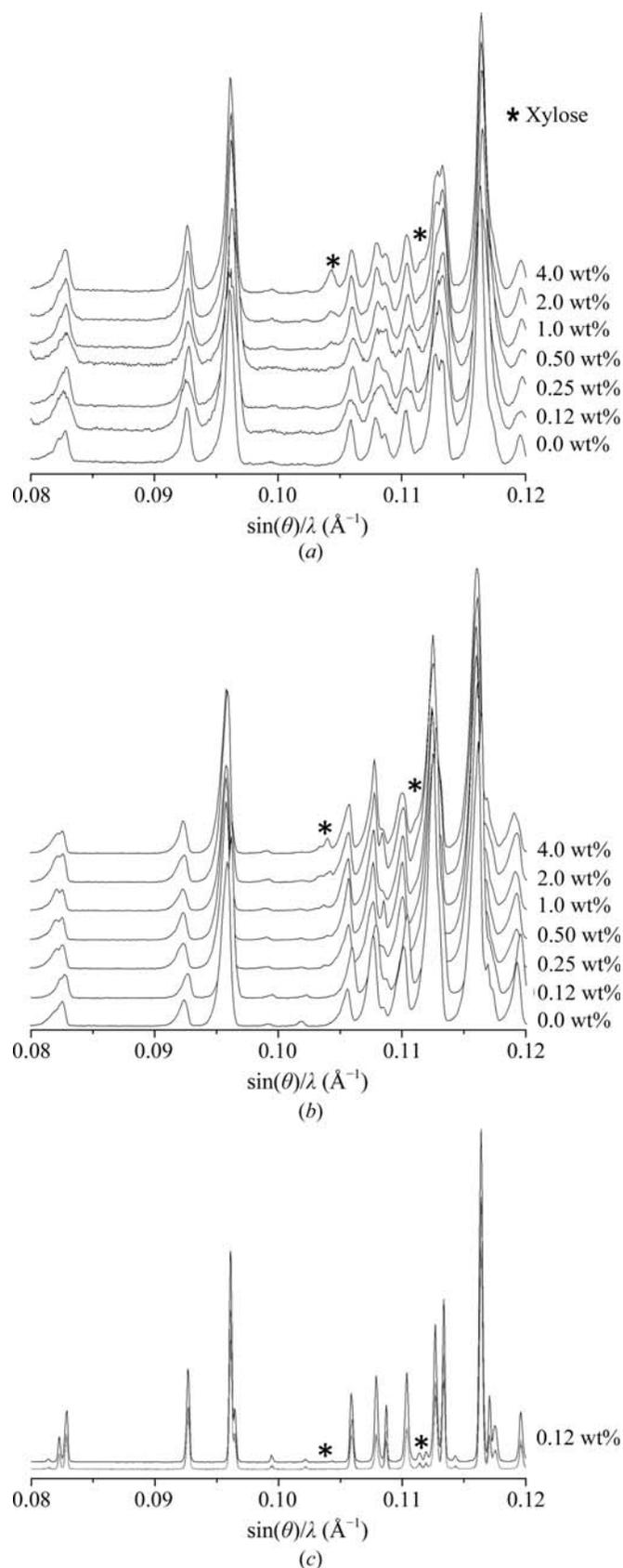
Figure 3.10.5

(*a*) Raw Mo $K\alpha_1$ powder patterns for the organic series composed of a constant matrix of glucose, fructose and lactose, and increasing amounts of xylose (peaks highlighted with an asterisk). (*b*) Raw Cu $K\alpha_1$ powder patterns for the same organic series. (*c*) Raw SXRPD patterns for GFL_0.12X collected at three different positions of the capillary (as collected).

using laboratory radiation. Moreover, the Mo $K\alpha_1$ radiation analyses were slightly better than those obtained using Cu $K\alpha_1$ radiation.